LECTURE 12: THE MEASUREMENT OF POWER SPECTRUM AND CORRELATION FUNCTION

GONG-BO ZHAO

Abstract. This lecture explains how the power spectrum and the two-point correlation function are measured from a realistic galaxy redshift survey. The compact 2025 derivations are kept intact. The 2026 extension adds more interpretation of FKP weighting, effective volume, anisotropic pair counts, practical weighted estimators, and optimal redshift weights for BAO distance measurements and RSD growth measurements.

Learning goals

After this lecture, students should be able to:

- derive the FKP weight and explain its connection to effective survey volume;
- write weighted estimators for the power spectrum and correlation function;
- distinguish isotropic pair counts from anisotropic pair counts in (s, μ) bins;
- explain why wide redshift surveys lose information when they are compressed to one effective redshift;
- construct the standard optimal redshift weights for BAO and RSD analyses.

1. The FKP weight

The FKP weight is the optimal weight for measurement of power spectrum multipoles [1].

$$P(k) = P(\mathbf{k}) \equiv \int d^3r \xi(\mathbf{r}) e^{i\mathbf{k}\cdot\mathbf{r}} \tag{1}$$

$$F(\mathbf{r}) \equiv \frac{w(\mathbf{r})\left[n_g(\mathbf{r}) - \alpha n_s(\mathbf{r})\right]}{\left[\int d^3r \overline{n}^2(\mathbf{r}) w^2(\mathbf{r})\right]^{1/2}} \tag{2}$$

$$\left\langle |F(\mathbf{k})|^2 \right\rangle = \frac{\int d^3r \int d^3r' w(\mathbf{r}) w\left(\mathbf{r}'\right) \left\langle \left[n_g(\mathbf{r}) - \alpha n_s(\mathbf{r})\right]\left[n_g\left(\mathbf{r}'\right) - \alpha n_s\left(\mathbf{r}'\right)\right]\right\rangle e^{i\mathbf{k}\cdot(\mathbf{r}-\mathbf{r}')}}{\int d^3r \overline{n}^2(\mathbf{r}) w^2(\mathbf{r})}$$

$$\begin{aligned} \left\langle n_g(\mathbf{r}) n_g\left(\mathbf{r}'\right)\right\rangle &= \overline{n}(\mathbf{r})\overline{n}\left(\mathbf{r}'\right)\left[1 + \xi\left(\mathbf{r} - \mathbf{r}'\right)\right] + \overline{n}(\mathbf{r})\delta\left(\mathbf{r} - \mathbf{r}'\right) \\ \left\langle n_s(\mathbf{r}) n_s\left(\mathbf{r}'\right)\right\rangle &= \alpha^{-2}\overline{n}(\mathbf{r})\overline{n}\left(\mathbf{r}'\right) + \alpha^{-1}\overline{n}(\mathbf{r})\delta\left(\mathbf{r} - \mathbf{r}'\right) \\ \left\langle n_g(\mathbf{r}) n_s\left(\mathbf{r}'\right)\right\rangle &= \alpha^{-1}\overline{n}(\mathbf{r})\overline{n}\left(\mathbf{r}'\right) \end{aligned} \tag{3}$$

$$\left\langle |F(\mathbf{k})|^2 \right\rangle = \int \frac{d^3k'}{(2\pi)^3} P\left(\mathbf{k}'\right) \left| G\left(\mathbf{k}-\mathbf{k}'\right)\right|^2 + (1+\alpha)\frac{\int d^3r\overline{n}(\mathbf{r})w^2(\mathbf{r})}{\int d^3r\overline{n}^2(\mathbf{r})w^2(\mathbf{r})} \tag{4}$$

$$G(\mathbf{k}) \equiv \frac{\int d^3r\overline{n}(\mathbf{r})w(\mathbf{r})e^{i\mathbf{k}\cdot\mathbf{r}}}{\left[\int d^3r\overline{n}^2(\mathbf{r})w^2(\mathbf{r})\right]^{1/2}} \tag{5}$$

$$\left\langle |F(\mathbf{k})|^2 \right\rangle \simeq P(\mathbf{k}) + P_{\rm shot} \tag{6}$$

$$P_{\rm shot} \equiv \frac{(1+\alpha)\int d^3r\overline{n}(\mathbf{r})w^2(\mathbf{r})}{\int d^3r\overline{n}^2(\mathbf{r})w^2(\mathbf{r})} \tag{7}$$

$$\hat{P}(\mathbf{k}) = |F(\mathbf{k})|^2 - P_{\rm shot} \tag{8}$$

$$\hat{P}(k) \equiv \frac{1}{V_k}\int_{V_k} d^3k'\hat{P}\left(\mathbf{k}'\right) \tag{9}$$

$$\sigma_P^2(k) \simeq \frac{1}{V_k}\int d^3k' \left| P(k)Q\left(\mathbf{k}'\right) + S\left(\mathbf{k}'\right)\right|^2 \tag{10}$$

where

$$Q(\mathbf{k}) \equiv \frac{\int d^3r\overline{n}^2(\mathbf{r})w^2(\mathbf{r})e^{i\mathbf{k}\cdot\mathbf{r}}}{\int d^3r\overline{n}^2(\mathbf{r})w^2(\mathbf{r})} \tag{11}$$

and

$$S(\mathbf{k}) \equiv \frac{(1+\alpha)\int d^3r\overline{n}(\mathbf{r})w^2(\mathbf{r})e^{i\mathbf{k}\cdot\mathbf{r}}}{\int d^3r\overline{n}^2(\mathbf{r})w^2(\mathbf{r})} \tag{12}$$

$$\frac{\sigma_P^2(k)}{P^2(k)} = \frac{(2\pi)^3\int d^3r\overline{n}^4w^4[1+1/\overline{n}P(k)]^2}{V_k\left[\int d^3r\overline{n}^2w^2\right]^2} \tag{13}$$

The KFP weight taking the following form minimises Eq (13):

$$w_0(\mathbf{r}) = \frac{1}{1+\overline{n}(\mathbf{r})P(k)} \tag{14}$$

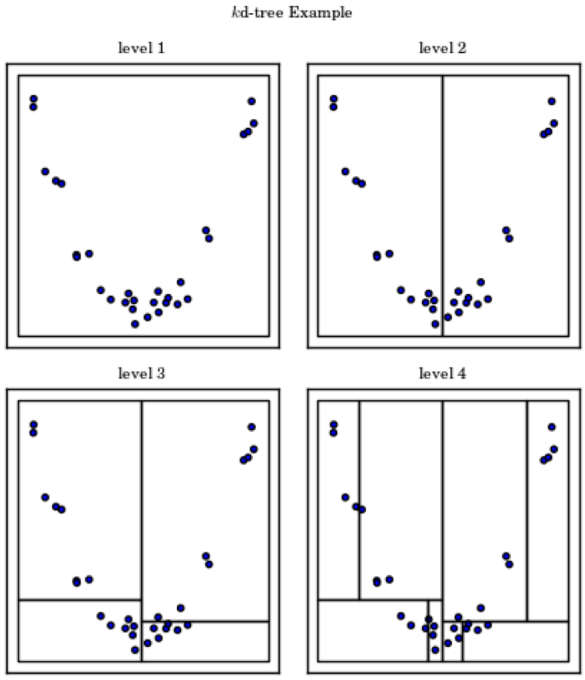

FIGURE 1. An example of kdtree.

2. The measurement of the anisotropic correlation function

Pair counts in 'data' are compared to pair counts in 'random' samples that follow the geometry of the survey. We assume a catalogue of n_d objects in the data sample and n_r in the random sample and then calculate three sets of numbers of pairs as a function of the binned comoving separation s,

```
function dualtree(node1, node2) {
  If node1 and node2 have already been compared in reverse
    return
  Let dmin = minimum distance between node1 and node2
  If dmin is greater than maximum distance of interest
    return
  Let dmax = maximum distance between node1 and node2
  Let binmin = distance bin for distance dmin
  Let binmax = distance bin for distance dmax
  If binmin = binmax
    Add node1.cnt x node2.cnt to bin count
  Else if node1 and node2 are leaf nodes
    For all points i owned by node1
      Let smin = minimum distance between point i and node2
      Let smax = maximum distance between point i and node2
      Let binmin = distance bin for smin
      Let binmax = distance bin for distance smax
      If binmin = binmax
        Add node2.cnt to bin count
      Else
        Find distances to all points in node2 from point i
        Find distance bins and update the bin counts
    Else
      If node1.cnt > node2.cnt
        dualtree(node1.leftChild, node2)
        dualtree(node1.rightChild, node2)
      Else
        dualtree(node1, node2.leftChild)
        dualtree(node1, node2.rightChild)
  }
```

FIGURE 2. The pseudo-code of kdtree.

- Data-data pairs $dd(s)$ that normalized by the total number of data pairs:

$$DD(s) = \frac{dd(s)}{n_d\left(n_d-1\right)/2}; \tag{15}$$

- Random-Random pairs $rr(s)$ that normalized by the total number of random pairs:

$$RR(s) = \frac{rr(s)}{n_r\left(n_r-1\right)/2}; \tag{16}$$

- Data-Random pairs $dr(s)$ that normalized by the total number of cross pairs:

$$DR(s) = \frac{dr(s)}{n_r n_d}. \tag{17}$$

The most commonly used Landy & Szalay estimator [4]:

$$\hat{\xi}(s) = \frac{DD - 2DR + RR}{RR}. \tag{18}$$

The task now is to compute the pair counts quickly for a large sample, which is challenging. For example, for BOSS DR12 sample, there are $\sim$ 1M data samples, and $\sim$ 100M random samples! So this is mission impossible for a brutal force algorithm with $O(N^2)$ complexity.

The way out is to use the kd-tree algorithm [1].

The kdtree code for the measurement: `https://github.com/wll745881210/KDTPCF`

The equations and discussion above are the compact material kept from the 2025 notes. The remaining sections extend the lecture in the more explanatory 2026 style.

3. More on the FKP estimator and effective volume

The FKP weight is often the first example of an optimal weighting rule in large-scale-structure analyses. The key idea is simple: a region of the survey is most useful when it has both a large volume and enough galaxies that shot noise is not dominant. If $\bar{n}P \gg 1$, adding more galaxies in that region does not help much because cosmic variance dominates. If $\bar{n}P \ll 1$, the same region is shot-noise dominated and should be downweighted.

For a fixed Fourier scale k, the FKP result can be rewritten in terms of an effective volume,

$$V_{\rm eff}(k) = \int d^3r \left[\frac{\bar{n}(\mathbf{r})P(k)}{1+\bar{n}(\mathbf{r})P(k)}\right]^2. \tag{19}$$

For a shell of width Δk, the approximate number of independent modes is

$$N_{\rm mode}(k) \simeq \frac{4\pi k^2 \Delta k}{(2\pi)^3} V_{\rm eff}(k), \tag{20}$$

[1] `http://www.linuxclustersinstitute.org/conferences/archive/2008/PDF/Dolence_98279.pdf`

and the usual Gaussian estimate gives

$$\frac{\sigma_P(k)}{P(k)} \simeq \sqrt{\frac{2}{N_{\rm mode}(k)}}. \tag{21}$$

This form is useful pedagogically because it shows what the FKP weight is doing: it converts an inhomogeneous survey into the volume of an ideal uniform survey with the same statistical power.

In real catalogues the total object weight is usually a product of several pieces,

$$w_{\rm tot}(\mathbf{r}) = w_{\rm sys}(\mathbf{r}) w_{\rm cp}(\mathbf{r}) w_{\rm zfail}(\mathbf{r}) w_{\rm FKP}(\mathbf{r}), \tag{22}$$

where $w_{\rm sys}$ corrects angular observational systematics, $w_{\rm cp}$ and $w_{\rm zfail}$ correct close-pair and redshift-failure effects, and

$$w_{\rm FKP}(\mathbf{r}) = \frac{1}{1+\bar{n}(\mathbf{r})P_\star} \tag{23}$$

uses a characteristic amplitude $P_\star$ near the scales of interest. For BAO-only work one often chooses $P_\star$ near the BAO scale, while for broadband power-spectrum work one may choose a value appropriate to the target range of k.

Example. If two survey regions have the same geometric volume, but one has $\bar{n}P_\star = 3$ and the other has $\bar{n}P_\star = 0.3$, then the FKP factors in $V_{\rm eff}$ are

$$\left(\frac{3}{1+3}\right)^2 = 0.5625, \qquad \left(\frac{0.3}{1+0.3}\right)^2 \simeq 0.053. \tag{24}$$

The sparse region contributes only about ten per cent as much effective volume as the dense region, even though the geometric volumes are identical.

The FKP idea can also be generalized to weights that depend on object properties, for example luminosity-dependent weights [6]. The optimal-redshift-weight methods introduced below are another generalization: instead of asking only how to weight volume against shot noise, they ask how to weight different redshifts according to their sensitivity to the cosmological parameter being measured.

4. Weighted pair counts and anisotropic correlation functions

The Landy–Szalay estimator written above is the isotropic version. In redshift-space distortion and anisotropic BAO analyses one counts pairs as a function of both separation and angle to the line of sight. For a pair at positions $\mathbf{x}_1$ and $\mathbf{x}_2$, define

$$\mathbf{s} = \mathbf{x}_2 - \mathbf{x}_1, \qquad s = |\mathbf{s}|, \qquad \hat{\mathbf{n}} = \frac{\mathbf{x}_1 + \mathbf{x}_2}{|\mathbf{x}_1 + \mathbf{x}_2|}, \qquad \mu = \hat{\mathbf{s}} \cdot \hat{\mathbf{n}}. \tag{25}$$

The anisotropic Landy–Szalay estimator is

$$\hat{\xi}(s,\mu) = \frac{DD(s,\mu) - 2DR(s,\mu) + RR(s,\mu)}{RR(s,\mu)}. \tag{26}$$

The multipoles are then

$$\hat{\xi}_\ell(s) = \frac{2\ell+1}{2}\int_{-1}^{1} d\mu\, \hat{\xi}(s,\mu)\mathcal{L}_\ell(\mu), \tag{27}$$

or, in a binned measurement,

$$\hat{\xi}_\ell(s) \simeq \frac{2\ell+1}{2}\sum_a \Delta\mu_a\, \hat{\xi}(s,\mu_a)\mathcal{L}_\ell(\mu_a). \tag{28}$$

For a parity-symmetric auto-correlation function, the odd multipoles vanish in the distant-observer limit. The monopole ξ_0 measures the angle-averaged clustering, the quadrupole ξ_2 is the leading redshift-space anisotropy, and the hexadecapole ξ_4 is useful for high-precision RSD modeling.

With object weights, the pair counts become weighted sums. For example,

$$DD(s,\mu) = \frac{\sum_{i<j\in D} w_i w_j\, \Theta_{ij}(s,\mu)}{\sum_{i<j\in D} w_i w_j}, \tag{29}$$

where $\Theta_{ij}(s,\mu)$ is one if the pair lies in the bin and zero otherwise. The corresponding DR and RR sums are defined analogously. This notation makes clear why the random catalogue must be passed through the same mask, radial selection, and redshift-dependent weights as the data.

5. Why redshift weights are useful

The FKP weight optimizes the measurement of a clustering statistic at a fixed scale, assuming the statistic itself is effectively constant across the survey volume. Wide surveys introduce a second question: how should we compress the smooth redshift evolution of the signal? Splitting the survey into many disjoint redshift bins gives tomographic information, but each bin has lower signal-to-noise and one discards pairs crossing the bin boundaries unless cross-bin statistics are included. Optimal redshift weights offer a compromise: keep the whole redshift range, but measure several weighted versions of the same statistic.

The general linear-compression result is straightforward. Suppose a data vector $\mathbf{x}$ has mean $\boldsymbol{\mu}(\boldsymbol{\theta})$ and covariance $\mathbf{C}$, and suppose $\mathbf{C}$ is treated as fixed. For one parameter θ_i, the Fisher information before compression is

$$F_{ii} = \boldsymbol{\mu}_{,i}^T \mathbf{C}^{-1} \boldsymbol{\mu}_{,i}. \tag{30}$$

A linear compressed datum

$$y_i = \mathbf{w}_i^T \mathbf{x} \tag{31}$$

is locally optimal if

$$\mathbf{w}_i \propto \mathbf{C}^{-1}\boldsymbol{\mu}_{,i}. \tag{32}$$

For several parameters one uses several weights, one for each derivative direction. This is the basic data-compression result of Tegmark, Taylor and Heavens [5], and it is the starting point for modern redshift-weighting schemes.

In a correlation-function analysis, the data vector may be the set of redshift-sliced correlation functions,

$$\mathbf{\Xi}(r) = (\xi(r, z_1), \xi(r, z_2), \ldots, \xi(r, z_N))^T . \tag{33}$$

A redshift-weighted correlation function is

$$\xi_w(r) = \mathbf{w}^T \mathbf{\Xi}(r). \tag{34}$$

If the redshift slices are treated as approximately independent, the inverse-covariance part contains the familiar FKP factor,

$$d\mathcal{W}(z) = \left[\frac{\bar{n}(z)}{1 + \bar{n}(z)P_\star}\right]^2 dV, \qquad dV = \frac{\chi_f^2(z)}{H_f(z)} dz\, d\Omega. \tag{35}$$

Thus the full redshift weight is conceptually the product of two pieces: an inverse-variance piece, controlled by $\bar{n}(z)$ and the survey volume, and a cosmological-sensitivity piece, controlled by the derivative of the model with respect to the target parameter.

6. Optimal BAO redshift weights

For BAO measurements, Zhu, Padmanabhan and White [7] proposed to parametrize the true distance-redshift relation relative to a fiducial relation by

$$\frac{\chi(z)}{\chi_f(z)} = \alpha_0 \left(1 + \alpha_1 x + \frac{1}{2}\alpha_2 x^2\right), \qquad 1 + x \equiv \frac{\chi_f(z)}{\chi_f(z_0)}. \tag{36}$$

The pivot redshift z_0 is chosen for convenience, usually near the pair-weighted effective redshift of the sample. At the pivot,

$$\alpha_0 = \frac{\chi(z_0)}{\chi_f(z_0)}, \tag{37}$$

while α_1 and α_2 describe the first and second derivative information in the distance-redshift relation.

The usual anisotropic BAO dilation variables are

$$\alpha_\perp(z) = \frac{\chi(z)}{\chi_f(z)}, \qquad \alpha_\parallel(z) = \frac{H_f(z)}{H(z)} = \frac{d\chi}{d\chi_f}. \tag{38}$$

Using the expansion above,

$$\alpha_\parallel(z) = \alpha_0 \left[1 + \alpha_1(1 + 2x) + \alpha_2 \left(x + \frac{3}{2}x^2\right)\right]. \tag{39}$$

Equivalently, using the isotropic dilation α and warping parameter ϵ,

$$\alpha(z) = \left[\alpha_\parallel(z)\alpha_\perp^2(z)\right]^{1/3}, \qquad 1 + \epsilon(z) = \left[\frac{\alpha_\parallel(z)}{\alpha_\perp(z)}\right]^{1/3}. \tag{40}$$

Working to linear order around the fiducial model, where $\alpha_0 = 1$ and $\alpha_1 = \alpha_2 = 0$, the derivatives are

$$\left.\frac{\partial\alpha}{\partial\alpha_0}\right|_0 = 1, \qquad \left.\frac{\partial\epsilon}{\partial\alpha_0}\right|_0 = 0, \tag{41}$$

$$\left.\frac{\partial\alpha}{\partial\alpha_1}\right|_0 = \frac{1}{3}(1+4x), \qquad \left.\frac{\partial\epsilon}{\partial\alpha_1}\right|_0 = \frac{1}{3}(1+x), \tag{42}$$

$$\left.\frac{\partial\alpha}{\partial\alpha_2}\right|_0 = \frac{1}{6}(2x+5x^2), \qquad \left.\frac{\partial\epsilon}{\partial\alpha_2}\right|_0 = \frac{1}{3}(x+x^2). \tag{43}$$

For BAO-only measurements, the leading response of the monopole is to α, while the leading response of the quadrupole is to ϵ. The redshift weights are therefore, up to arbitrary normalization,

$$w_{0,\alpha_0}(z) = 1, \qquad w_{2,\alpha_0}(z) = 0, \tag{44}$$

$$w_{0,\alpha_1}(z) = \frac{1}{3}(1+4x), \qquad w_{2,\alpha_1}(z) = \frac{1}{3}(1+x), \tag{45}$$

$$w_{0,\alpha_2}(z) = \frac{1}{6}(2x+5x^2), \qquad w_{2,\alpha_2}(z) = \frac{1}{3}(x+x^2). \tag{46}$$

The weighted correlation-function multipoles can be written as

$$\xi_{w,\ell,i}(s) = \frac{1}{N}\int d\mathcal{W}(z)\, w_{\ell,\alpha_i}(z)\xi_\ell(s,z), \qquad N = \int d\mathcal{W}(z). \tag{47}$$

The $i = 0$ mode is close to the usual single-effective-redshift BAO measurement. The $i = 1$ and $i = 2$ modes are redshift-gradient and redshift-curvature measurements, and they recover tomographic information without hard redshift slicing.

A pair-count implementation follows directly from Landy–Szalay. In redshift slices one may define

$$\widetilde{DD}_{\ell,i}(s) = \sum_z w_{\ell,\alpha_i}(z) w^2_{\rm FKP}(z) DD_z(s), \tag{48}$$

$$\widetilde{DR}_{\ell,i}(s) = \sum_z w_{\ell,\alpha_i}(z) w^2_{\rm FKP}(z) DR_z(s), \tag{49}$$

$$\widetilde{RR}_{\ell,i}(s) = \sum_z w_{\ell,\alpha_i}(z) w^2_{\rm FKP}(z) RR_z(s), \tag{50}$$

and then form

$$\hat{\xi}_{\ell,i}(s) = \frac{\widetilde{DD}_{\ell,i}(s) - 2\widetilde{DR}_{\ell,i}(s) + \widetilde{RR}_{\ell,i}(s)}{RR_{\rm FKP}(s)}. \tag{51}$$

Equivalently, one can assign each pair an additional weight $w_{\ell,\alpha_i}(z_{\rm pair})$, where $z_{\rm pair}$ is usually the mean redshift of the two objects. This works because the weights vary only on cosmological redshift scales, much more slowly than the BAO separation. Zhu *et al.* applied these weights to mock catalogues and showed how to fit the covariance between the weighted measurements [8].

7. Optimal redshift weights in Fourier space

The same idea can be used for power-spectrum multipoles. One measures a set of redshift-weighted multipoles,

$$P_{\ell,i}(k) = \int dz\, W_i(z) P_\ell(k,z), \tag{52}$$

where $W_i(z)$ includes the inverse-variance factor and the cosmological-sensitivity factor. In practice, one builds weighted galaxy and random fields and applies the same FFT-based machinery as in the previous lecture. A useful schematic form is

$$F_i(\mathbf{r}) = \frac{w_{\rm tot}(\mathbf{r}) q_i[z(\mathbf{r})]}{I_i^{1/2}} \left[n_g(\mathbf{r}) - \alpha n_s(\mathbf{r})\right], \tag{53}$$

with

$$I_i = \int d^3r\, \bar{n}^2(\mathbf{r}) w_{\rm tot}^2(\mathbf{r}) q_i^2[z(\mathbf{r})]. \tag{54}$$

Here $q_i(z)$ is the catalogue-level redshift weight used to realize the desired pair or power-spectrum weight. Practical Fourier-space BAO analyses often linearly transform the theoretical weight basis into positive modes and then assign the square root of the redshift weight to each object [10]. The transformation is linear, so the information content is preserved, and the covariance must be estimated for the transformed set of measured spectra.

For a set of measured weighted spectra, the covariance has an enlarged index structure,

$$C_{ij,ab}^{\ell\ell'} = \left\langle \left[P_{\ell,a}(k_i) - \bar{P}_{\ell,a}(k_i)\right] \left[P_{\ell',b}(k_j) - \bar{P}_{\ell',b}(k_j)\right] \right\rangle, \tag{55}$$

where a, b label the redshift weights. This covariance is usually estimated from mocks with the same weights applied to the mocks and the data.

8. Optimal redshift weights for RSD

For RSD, the target is usually the evolution of the growth rate, commonly summarized by $f\sigma_8(z)$. Ruggeri *et al.* [9] extended the redshift-weighting idea from BAO distances to RSD growth measurements. A convenient parametrization is an expansion of the matter fraction around a fiducial model,

$$\frac{\Omega_m(z)}{\Omega_{m,\rm fid}(z)} = q_0 \left(1 + q_1 y + \frac{1}{2} q_2 y^2\right), \qquad 1 + y \equiv \frac{\Omega_{m,\rm fid}(z)}{\Omega_{m,\rm fid}(z_p)}. \tag{56}$$

The pivot redshift z_p is again a convenient choice near the centre of the survey. The parameters q_0, q_1, q_2 describe the amplitude, slope and curvature of deviations from the fiducial growth and expansion history.

In linear theory,

$$P^s(k,\mu,z) = \left[b(z) + f(z)\mu^2\right]^2 P_m(k,z), \tag{57}$$

and the first three even multipoles are

$$P_0(k,z) = \left[b^2 + \frac{2}{3}bf + \frac{1}{5}f^2\right] P_m(k,z), \tag{58}$$

$$P_2(k,z) = \left[\frac{4}{3}bf + \frac{4}{7}f^2\right] P_m(k,z), \tag{59}$$

$$P_4(k,z) = \left[\frac{8}{35}f^2\right] P_m(k,z). \tag{60}$$

If the bias is treated as unknown and marginalized over, the growth information is carried mainly by $f\sigma_8(z)$. Writing $B(z) = b(z)\sigma_8(z)$ and $F(z) = f(z)\sigma_8(z)$, the RSD redshift weights are proportional to

$$w_{0,q_i}(z) = \left[\frac{2}{3}B(z) + \frac{2}{5}F(z)\right] \frac{\partial F(z)}{\partial q_i}, \tag{61}$$

$$w_{2,q_i}(z) = \left[\frac{4}{3}B(z) + \frac{8}{7}F(z)\right] \frac{\partial F(z)}{\partial q_i}, \tag{62}$$

$$w_{4,q_i}(z) = \left[\frac{16}{35}F(z)\right] \frac{\partial F(z)}{\partial q_i}. \tag{63}$$

These expressions should be read together with the inverse-variance factor, just as in the BAO case. The weights are not universal: a weight optimized for $f\sigma_8$ is different from one optimized for a BAO dilation parameter, and both are different from a weight optimized for primordial non-Gaussianity or another scale-dependent effect.

Interpretation. The monopole weight contains both density and velocity information, the quadrupole weight is more directly sensitive to anisotropic RSD, and the hexadecapole weight is proportional to $F(z)\partial F/\partial q_i$. The hexadecapole is therefore valuable in principle, but in real surveys it often has lower signal-to-noise than the monopole and quadrupole.

9. Effective redshift and weighted models

For an ordinary unweighted measurement, one often quotes a pair-weighted effective redshift,

$$z_{\rm eff} = \frac{\sum_{\rm pairs} w_a w_b z_{ab}}{\sum_{\rm pairs} w_a w_b}, \qquad z_{ab} = \frac{z_a + z_b}{2}. \tag{64}$$

For a redshift-weighted measurement one can formally define

$$z_{{\rm eff},i} = \frac{\int d\mathcal{W}(z) w_i(z) z}{\int d\mathcal{W}(z) w_i(z)}. \tag{65}$$

This is useful for intuition, but it can be misleading when $w_i(z)$ changes sign. In that case the denominator can be small, and the resulting number may not represent where the information really comes from. The safer procedure is to compare the measurement to a

redshift-weighted theoretical model,

$$M_i = \frac{1}{N_i} \int d\mathcal{W}(z) w_i(z) M(z), \tag{66}$$

rather than evaluating an unweighted model at a single effective redshift.

10. Practical workflow

A realistic redshift-weighted clustering analysis can be summarized as follows:

(1) choose the cosmological quantities to optimize, such as $\alpha_0, \alpha_1, \alpha_2$ for BAO or q_0, q_1, q_2 for RSD;
(2) choose a fiducial cosmology and pivot redshift;
(3) compute the redshift weights from model derivatives and inverse-variance factors;
(4) apply the same redshift weights to data, randoms and mocks;
(5) measure the set of weighted $\xi_\ell(s)$ or $P_\ell(k)$ statistics;
(6) estimate the full covariance matrix, including correlations between different redshift weights;
(7) fit the compressed parameters and reconstruct $D_A(z)$, $H(z)$, and/or $f\sigma_8(z)$ over the survey redshift range.

The essential advantage is that the analysis avoids arbitrary hard redshift bins while retaining sensitivity to smooth evolution across the light cone. Zhao *et al.* used this logic for tomographic measurements of expansion and growth in the eBOSS quasar sample [11].

Summary

The FKP weight optimizes the trade-off between sample variance and shot noise. Landy–Szalay pair counts then provide a robust configuration-space estimator, and the anisotropic version leads naturally to correlation-function multipoles. Optimal redshift weights add a second layer of compression: instead of assuming that the whole survey is represented by one effective redshift, they measure smooth redshift modes of BAO distances or RSD growth. This makes the lecture's power-spectrum and correlation-function estimators directly applicable to modern wide-redshift surveys.

Suggested reading

- Feldman, Kaiser and Peacock [1] for the original power-spectrum weighting argument.
- Landy and Szalay [4] for the minimum-variance two-point correlation-function estimator.
- Tegmark, Taylor and Heavens [5] for optimal linear data compression.
- Zhu, Padmanabhan and White [7] and Zhu *et al.* [8] for BAO redshift weights.
- Ruggeri *et al.* [9] for RSD redshift weights.
- Wang *et al.* [10] and Zhao *et al.* [11] for applications to eBOSS quasar clustering.

Homework

(1) **Effective volume.** Starting from the FKP weight, derive $V_{\rm eff}(k)$ and explain the limiting behaviour when $\bar{n}P \gg 1$ and when $\bar{n}P \ll 1$.
(2) **Anisotropic pair counts.** Write pseudo-code for measuring $DD(s,\mu)$, $DR(s,\mu)$ and $RR(s,\mu)$ using weighted pair counts.
(3) **Effective redshift.** Explain why a sign-changing redshift weight should be compared to a redshift-weighted model rather than to a model evaluated at one effective redshift.

References

[1] H. A. Feldman, N. Kaiser and J. A. Peacock, "Power spectrum analysis of three-dimensional redshift surveys," Astrophys. J. **426**, 23 (1994) doi:10.1086/174036 [astro-ph/9304022].

[2] D. Bianchi, H. Gil-Marín, R. Ruggeri and W. J. Percival, "Measuring line-of-sight dependent Fourier-space clustering using FFTs," Mon. Not. Roy. Astron. Soc. **453**, no. 1, L11 (2015) doi:10.1093/mnrasl/slv090 [arXiv:1505.05341 [astro-ph.CO]].

[3] N. Hand, Y. Li, Z. Slepian and U. Seljak, "An optimal FFT-based anisotropic power spectrum estimator," JCAP **1707**, no. 07, 002 (2017) doi:10.1088/1475-7516/2017/07/002 [arXiv:1704.02357 [astro-ph.CO]].

[4] S. D. Landy and A. S. Szalay, "Bias and variance of angular correlation functions," Astrophys. J. **412**, 64 (1993). doi:10.1086/172900

[5] M. Tegmark, A. N. Taylor and A. F. Heavens, "Karhunen-Loeve eigenvalue problems in cosmology: How should we tackle large data sets?," Astrophys. J. **480**, 22 (1997) doi:10.1086/303939 [astro-ph/9603021].

[6] W. J. Percival, L. Verde and J. A. Peacock, "Fourier analysis of luminosity-dependent galaxy clustering," Mon. Not. Roy. Astron. Soc. **347**, 645 (2004) doi:10.1111/j.1365-2966.2004.07245.x [astro-ph/0306511].

[7] F. Zhu, N. Padmanabhan and M. White, "Optimal redshift weighting for baryon acoustic oscillations," Mon. Not. Roy. Astron. Soc. **451**, no. 1, 236 (2015) doi:10.1093/mnras/stv964 [arXiv:1411.1424 [astro-ph.CO]].

[8] F. Zhu, N. Padmanabhan, M. White, A. J. Ross and G.-B. Zhao, "Redshift weights for baryon acoustic oscillations: Application to mock galaxy catalogues," Mon. Not. Roy. Astron. Soc. **461**, no. 3, 2867 (2016) doi:10.1093/mnras/stw1515 [arXiv:1604.01050 [astro-ph.CO]].

[9] R. Ruggeri, W. J. Percival, H. Gil-Marín, F. Zhu, G.-B. Zhao and Y. Wang, "Optimal redshift weighting for redshift-space distortions," Mon. Not. Roy. Astron. Soc. **464**, no. 3, 2698 (2017) doi:10.1093/mnras/stw2422 [arXiv:1602.05195 [astro-ph.CO]].

[10] D. Wang, G.-B. Zhao, Y. Wang, W. J. Percival, R. Ruggeri, F. Zhu, R. Tojeiro *et al.*, "The clustering of the SDSS-IV extended Baryon Oscillation Spectroscopic Survey DR14 quasar sample: anisotropic Baryon Acoustic Oscillations measurements in Fourier-space with optimal redshift weights," Mon. Not. Roy. Astron. Soc. **477**, no. 2, 1528 (2018) doi:10.1093/mnras/sty654 [arXiv:1801.03077 [astro-ph.CO]].

[11] G.-B. Zhao, Y. Wang, S. Saito, H. Gil-Marín, W. J. Percival, D. Wang, C.-H. Chuang *et al.*, "The clustering of the SDSS-IV extended Baryon Oscillation Spectroscopic Survey DR14 quasar sample: a tomographic measurement of cosmic structure growth and expansion rate based on optimal redshift weights," Mon. Not. Roy. Astron. Soc. **482**, no. 3, 3497 (2019) doi:10.1093/mnras/sty2845 [arXiv:1801.03043 [astro-ph.CO]].